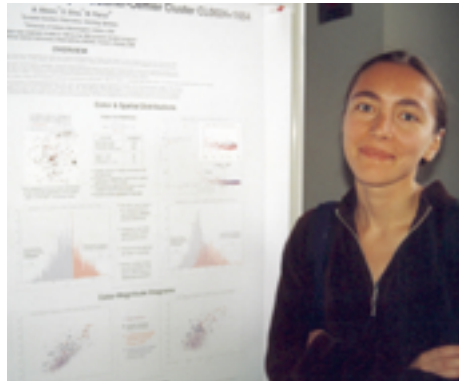


A WIDE-FIELD, BROAD BAND IMAGING SURVEY OF BUTCHER-OEMLER CLUSTER CL0024+1654



A. Alexov (1), D. Silva (1), M. Pierce (2)

(1) *European Southern Observatory, Karl-Schwarzschild-Str. 2, D-85748 Garching, Germany*

(2) *Univeristy of Indiana, 107 S. Indiana Ave., Bloomington, IN 47405-7000, USA*

A wide-field imaging study of intermediate-redshift ($z = 0.39$), Butcher-Oemler cluster CL0024+1654 has been initiated. Previous studies of the galaxy population of this cluster have concentrated only on the most centrally located galaxies. To improve this situation, wide-field (20 x 20 arcmin) UBVI images have been obtained. In this poster, a preliminary analysis of this dataset is presented. In particular, the color and spatial distributions of the galaxies are used to discuss the nature of the intra-cluster “faint blue” galaxy population and extent to which CL0024+1654 is embedded in a larger super-cluster complex. An analysis of optical band “drop-out” objects, candidates for high-redshift galaxies, is also presented. These data are deep enough ($S/N = 5$ at $B = 24.5$) that the luminosity function of the elliptical, S0, and spiral galaxies is sampled well enough to investigate population differences within a class as a function of luminosity/mass. This part of the analysis has not been completed and it is not discussed further here.

1 Introduction

This poster presents the preliminary results of a wide-field imaging study of intermediate-redshift ($z = 0.39$), Butcher-Oemler cluster CL0024+1654. Previous studies of the galaxy population of this cluster have concentrated only on the most centrally located galaxies. To improve this situation, we have obtained wide-field (20 x 20 arcmin) UBVI images. At this redshift, UBVI correspond to two mid-UV (2500Å and 3000Å) and two optical (B and R) bandpasses in the cluster rest-frame. Our main objective was to study and compare the cluster and field galaxy populations. Given the extreme field/cluster density contrast and a 20 arcmin field-of-view, purely statistical arguments can be used to establish cluster membership. These data are directly relevant to issues regarding the origin and evolution of faint blue galaxies, and the question of whether CL0024+1654 is embedded in a more extended supercluster complex. In particular, we have investigated whether the faint blue field population has an intra-cluster analogue. This dataset is also deep enough ($S/N = 5$ at $B = 24.5$), covers a large enough area, and contains enough color information to provide an interesting set of photometric “drop out” objects, i.e. potential high-redshift objects. We present some preliminary statistics and examples. Looking ahead, our dataset contains the necessary color information to distinguish between the “E+S0”, “E+A”, and spiral/irregular galaxy populations throughout the cluster/supercluster complex. The rest-frame colors provide a powerful “blue” galaxy discriminate given the expected color

distribution. Moreover, since “hot” stars peak near 2500\AA , that bandpass is a powerful probe of recent star formation activity in all classes of galaxies. In particular, it is sensitive to ellipticals (objects with red B-R rest-frame colors) with “UV excess” populations. By going deep, we are sampling the luminosity function of the elliptical, S0, and spiral galaxies well enough to investigate population differences within a class as a function of luminosity/mass. We have not completed this part of our analysis and it is not discussed further here.

2 Data Acquisition and Processing

2.1 Observations

CL0024+1654 was observed with the NOAO Kitt Peak National Observatory 0.9m telescope in Sept. 1991, Oct. 1991 and Sept. 1992. The data were taken with the “Harris” UBVI standard filter set, using the T2KA and T2KB CCD cameras. The mean cluster redshift is known to be $z = 0.39^4$, although more recent spectroscopic work has separated CL0024+1654 into two sub-clusters at $z = 0.3949$ and $z = 0.383^3$.

2.2 Data Reduction

Using various tasks in IRAF, the raw images were bias subtracted, flat fielded, and illumination corrected. The I band frames were fringe corrected. Because the data were taken on scattered nights within the period of one year, with different CCD’s and different filters, the data had to be transformed to the same image scale and size. Then the images were combined to increase signal-to-noise for the individual filters. Magnitudes were transformed to the Landolt (1993) system. The final data products were U, B, V, and I images of CL0024+1654. All subsequent analysis was done on these four images.

2.3 Object Catalog Construction

Source Extractor (SExtractor)¹ was used to find all the objects significantly above sky background noise, classify these objects as either galactic stars or distant galaxies and measure the brightness of all these detected objects. Cluster galaxies span a large color range. These galaxies can also have color gradients which cause the same object to have seemingly different morphologies in different filters. These complications made the SExtractor tasks more difficult to accomplish since the images were taken through filters which isolate light of very specific wavelengths. Hence, unassisted, SExtractor will tend to detect blue objects as well as blue parts of galaxies in the “blue” (U and B) images and red objects as well as red parts of galaxies in the “red” (V and I) images. To assure that galaxies of all colors were detected in an unbiased manner as well as to make sure that the brightness of each object was measured within the same physical area on each image, a “U+B+V+I” image was created, simulating the effect of imaging through a much broader filter. We used the IRAF GAUSS routine to bring all the PSF’s to the same value, subtracted the median background value from each image and added all four filters together. This “UBVI” image contained galaxies of all colors as well as light from areas of different colors within the same object. SExtractor was run on the UBVI image for detection of objects. The detection threshold, deblending and background parameters were adjusted until the visual inspection of the results indicated an acceptable fit to the data. The center of CL0024+1654 is quite crowded; we wanted to make sure that obvious multi-object areas were being deblended correctly; the field also contains several bright stars and light streaks from bright stars - we had to chose background parameters appropriately to deal with these problem areas. SExtractor detected sources 1.7 sigma above the sky threshold, deblended any objects which were close together and determined a physical photometric aperture which encompassed

Table 1: SExtractor Output Catalog Statistics

<i>Category</i>	<i>Number of Objects</i>
Total objects detected	5992
Stars with a magnitude error in all 4 filters < 0.1 magnitudes	168
Galaxies within the total field-of-view having a magnitude error in all 4 filters < 0.2 magnitudes	1736
Galaxies within the total field-of-view having a magnitude error in all 4 filters < 0.33 magnitudes	2948
Galaxies within the main cluster (within 2.3 arcmins of image center) having a magnitude error in all 4 filters < 0.2 magnitudes	134
Galaxies within the main cluster (within 2.3 arcmins of image center) having a magnitude error in all 4 filters < 0.33 magnitudes	217

all the light from the object. Lastly SExtractor classified each object as either a star or a galaxy using it's builtin multi-layered neural network architecture.

Once the UBVI isophote apertures were created, we used these same apertures on the individual U, B, V and I images. SExtractor found 6136 objects and assigned each one an isophotal magnitude and an aperture (rad=2.5 pixels) magnitude in each of the 4 filters for CL0024. These detections were inspected visually; 144 were removed for being close to the edge of the image, in the halo of a bright star or in the off-field reflections of bright sources. The final catalog contained 5992 sources which are used for the analysis and discussion below. The SExtractor catalog results can be found in Table 1.

Please note: all further galaxy analysis is on data for which the magnitude error is < 0.2 in all 4 filters, corresponding approximately to $(UBVI) = (23, 24, X, 23)$. Note that these cut-offs are bright enough that our results will be unaffected by possible object depletion caused by gravitation lensing⁶.

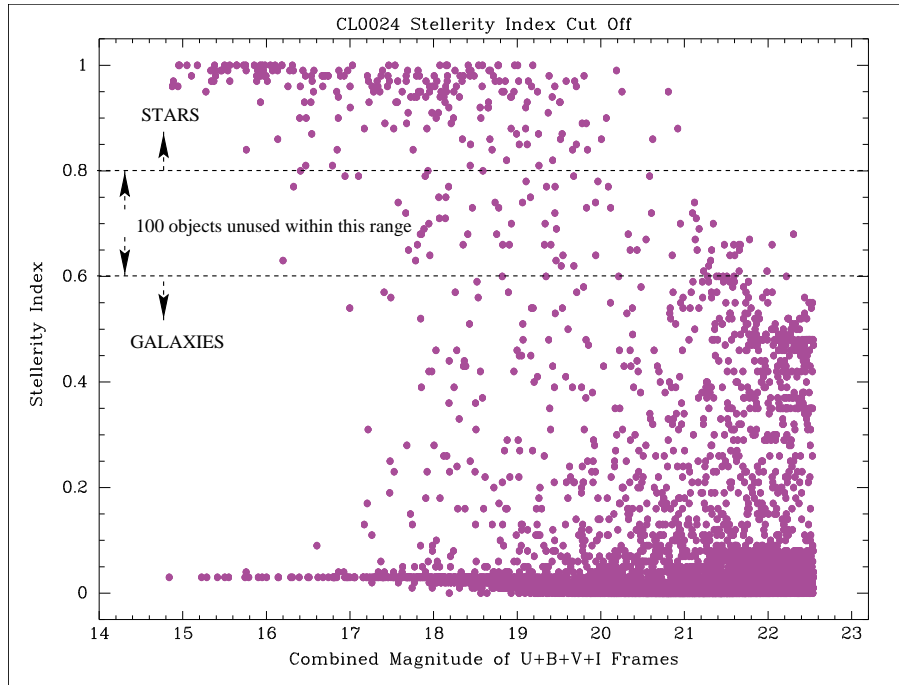


Figure 1: UBVI Magnitude plotted vs the Stellerity Index calculated by SExtractor. Objects with stellerity > 0.8 have been designated as stars, while objects with stellerity < 0.6 have been designated as galaxies. The ≈ 100 objects which fall in between 0.8 and 0.6 have been left out of our statistics since their classification is uncertain.

2.4 Star/Galaxy Separation

SExtractor’s star/galaxy separation output parameter is called the stellerity index; an object which is a star gets a value close to 1.0 vs 0.0 for an object which is a galaxy. It is up to the user to chose the cut off stellerity index which separates the stars and galaxies in the data. Since the shape of a galaxy can change in the individual U,B,V and I filter frames, the combined UBVI image was used to determine the stellerity cut off. Using this frame ensures that all the light for all objects is used to classify it as a galaxy or a star. Figure 1 shows the object stellerity vs UBVI isophotal mag, for all the catalog objects which have isophotal magnitude errors less than 0.2 , and for which the “error reporting flags” were set less than 4^1 .

We decided that a stellerity cut off greater than 0.8 was suitable for stars and a stellerity less than 0.6 was suitable for galaxies. There are approximately 100 objects which fall in between stellerity 0.8 and 0.6 ; these objects are probably galaxies, but it is difficult to be certain, therefore these objects were ignored in subsequent analysis.

To check the stellerity index we compared the photometry of objects in the field with stellerity > 0.8 (stars) to bright nearby stars with well determined colors (Landolt standards) using color-color diagrams. Figure 2 is a superposition of 3 U-B vs. B-I graphs: Landolt standards are plotted as black dots, objects classified as stars in the field of CL0024+1654 are plotted as open blue circles and objects classified as galaxies by SExtractor are small magenta closed circles. This figure clearly shows that stars in the field tightly fit the Landolt standards while the galaxies are in different locations away from the stars. There is some overlap of stars and galaxies due to incorrect classification (round galaxies could have been classified as stars and faint stars could have been classified as galaxies), but overall, Figure 2 gives us confidence that the photometry and classification of objects in the CL0024+1654 fields are correct for the vast majority of

¹Only objects with no error reporting or ones which were originally blended or those with bright neighbors or those with 10% bad pixels are accepted into the catalog.

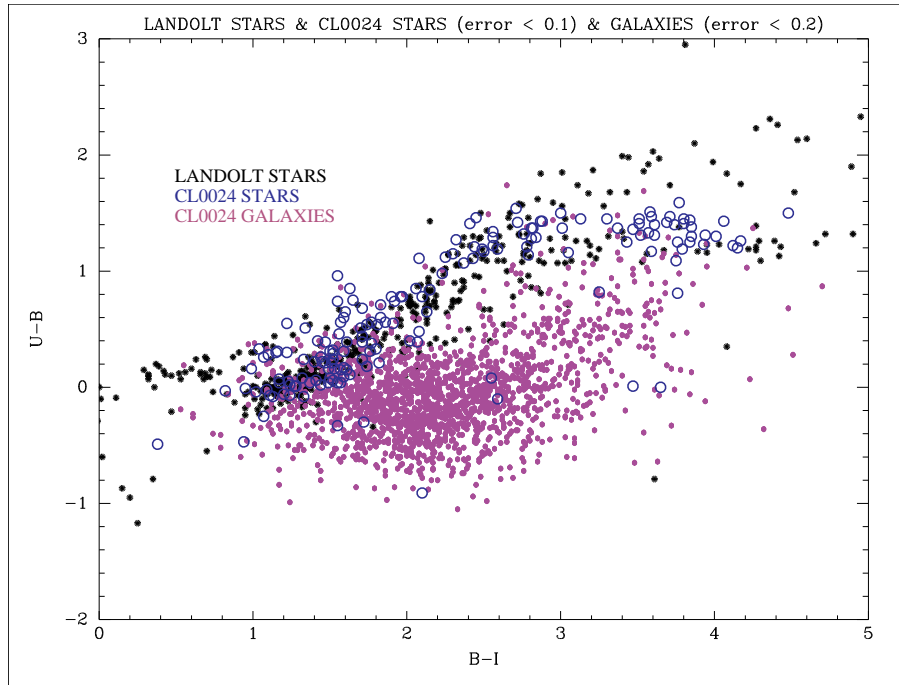


Figure 2: A superposition of 3 U-B vs B-I graphs: Landolt standards are plotted as black dots, objects classified as stars in the field of CL0024+1654 are plotted as open blue circles and objects classified as galaxies by SExtractor are small magenta closed circles. The stars in the field tightly fit the Landolt standards while the galaxies are in different locations away from the stars.

objects. The relatively small number of galaxies mis-classified as stars is a small effect which is not detrimental in our large statistical study.

3 Data Analysis

3.1 Color and Spatial Distribution

A color-cut was made on the final catalog, in order to separate the “blue” from the “red” galaxies in CL0024. The criteria used were:

- **Blue** objects have $B-V \leq 1.0$
- **Faint Blue** objects have $B-V \leq 1.0$ and $B \geq 22.0$
- **Red** objects have $B-V > 1.0$

The resultant color-cut statistics can be viewed in Table 2. This table shows the breakdown of the blue and red objects for the entire field of view as well as just for CL0024+1654 (radius from center less than 2.3 arcmins). The numbers suggest that there is a significant “faint blue” population in the cluster.

CL0024+1654 is a well-known Butcher-Oemler cluster⁴. This is illustrated in Figure 3 which provides a visual representation of the red and blue galaxy distribution in the CL0024+1654 cluster center region (within 2.3 arcmins). Blue galaxies are marked with blue boxes, while red galaxies are marked with red circles. The light-aqua rings are placed at approximately 5” radii out to 70” from center. There is clearly an even distribution of red and blue galaxies in the cluster. This also true for the field (not shown here).

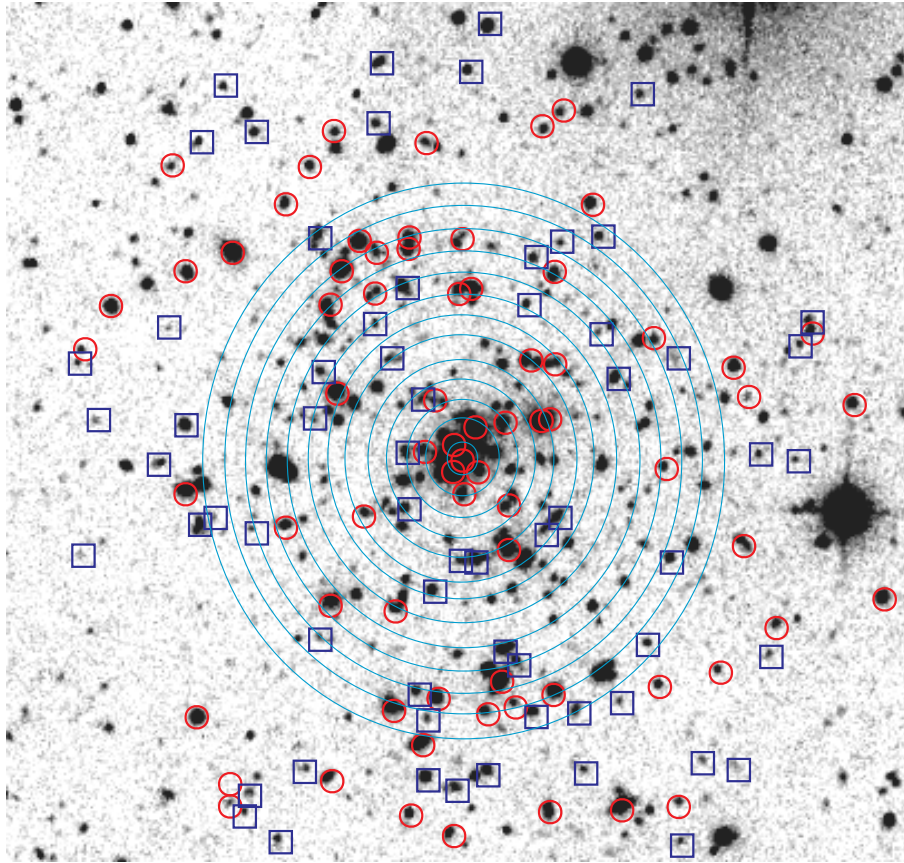


Figure 3: 2D image of the cluster center region of CL0024+1654 (within 2.3 arcmins of center). Blue galaxies are marked with blue boxes, while red galaxies are marked with red circles. The light-aqua rings are placed at approximately 5" radii out to 70" from center. There appears to be an even distribution of "red" and "blue" objects in this image.

Table 2: Color cut statistics for the entire CL0024+1654 field-of-view and for the center region.

<i>Color</i>	<i>Number</i>
Blue (entire field)	1106
Faint Blue (entire field)	975
Red (entire field)	630
Blue (center radius < 2.3 arcmins)	64
Faint Blue (center radius < 2.3 arcmins)	57
Red (center radius < 2.3 arcmins)	70

One of the goals of this project is to determine whether CL0024+1654 contains an intra-cluster analogue to the field faint blue galaxy population that peaks near this redshift. This question can be address statistically by determining the radial distribution of faint blue galaxies in this field, i.e. to measure the galaxy number density as a function of distance from the cluster center. The radial profile of CL0024+1654 is shown in Figure 4. The tail end of the distribution is enlarged in the sub-figure inside Figure 4. Clearly, the number density of both both red and blue galaxies declines with radius until it reaches some mean field density. It is also seen that the number density of faint blue galaxies is larger within CL0024+1654 than in the field. We infer that these intra-cluster faint blue galaxies galaxies are physically associated with CL0024+1654. Confirmation of this will require acquiring time-intensive redshifts for these objects using large aperture telescopes. There is also a 2nd peak in the distribution at 70" from center, which most likely indicates the of 2nd cluster³.

Histograms of the B–V and B–I color-cut are shown in Figure 5 and Figure 6, respectively. Since the color cut is made at B–V = 1, the B–I color shows a different blue/red distribution. These distributions highlight objects with extreme colors, noted by the dotted boxes; these objects are interesting candidates for further study and spectroscopic followup.

3.2 Color-Magnitude Diagrams

Two color magnitude diagrams are shown in Figures 7 and 8. Field galaxies are plotted in magenta, cluster galaxies (within 2.3 arcmins of center) are plotted in black; overplotted as blue and red open stars, are the confirmed CL0024+1654 cluster members⁴. All the confirmed members are bright with respect to the rest of our survey, and hence show up on the upper/brighter end of the plots.

3.3 Color-Color Diagrams

U–B vs B–I color-color diagram for the CL0024+1654 “field” and “center” are presented in Figures 9 and 10, respectively. The starred galaxies in Figure 10 are known, bright cluster members, all having $z \approx 0.4$ ⁴.

These color-color distributions can be compared to simulated galaxy spectral energy distributions (SEDs), appropriately redshifted. Simulated SEDs were constructed for a range of local epoch galaxy types, using the GISSEL system². The types of galaxies simulated ranged from young, irregular, star forming galaxies to old, non-star forming, red elliptical and SO galaxies. The current epoch spectra were then redshifted to values of $z = 0.2, 0.4, \dots, 1.0$. At each redshift, the galaxy colors in the observation frame were computed. The resultant color tracks are overplotted in the CL0024+1654 color-color diagrams. On each track, the bluest point corresponds to actively star forming irregular galaxy (e.g. NGC 4449) while the reddest point corresponds

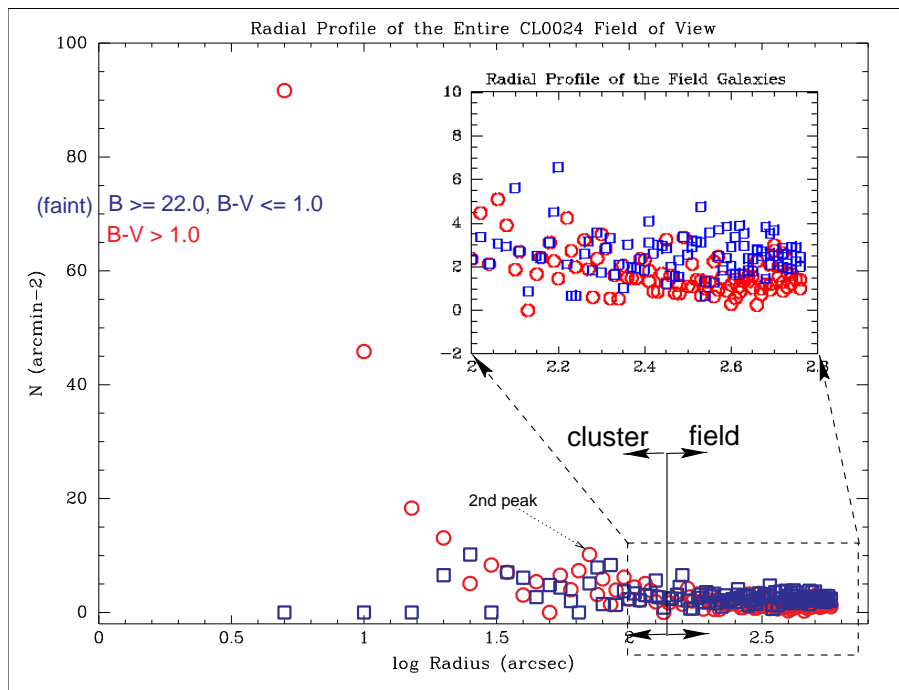


Figure 4: The radial profile of galaxies in CL0024+1654. The tail end of the distribution is enlarged in the sub-figure. As radial distance increases, both red and blue galaxies number density declines until a field plateau values is reached. Note the enhancement of faint blue galaxies within the cluster, at approximately twice the level of red galaxies.

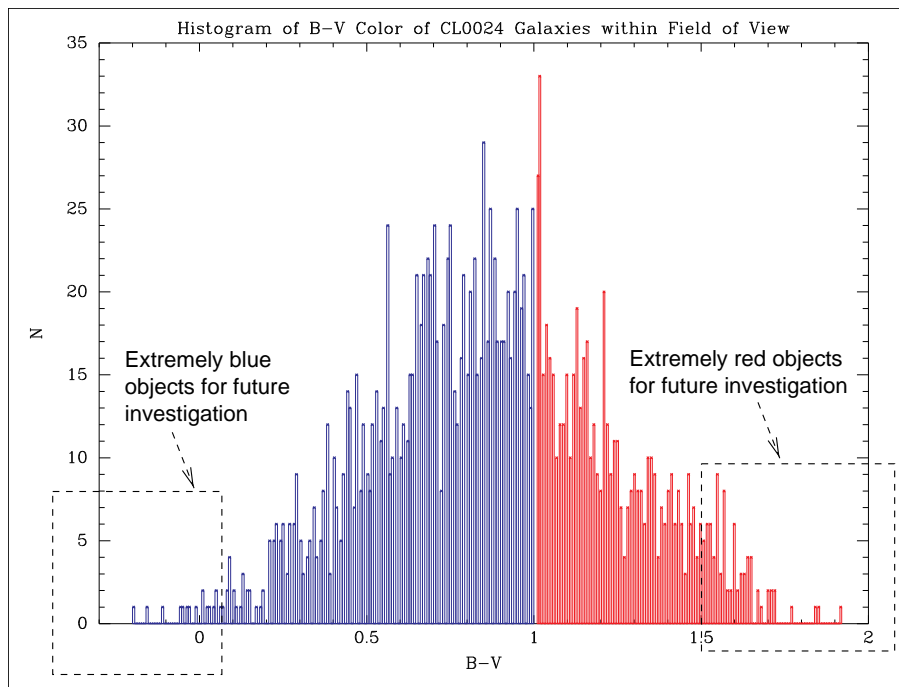


Figure 5: Histogram of the B-V color cut for galaxies in CL0024+1654. Objects with extreme colors are shown in dotted boxes. Objects are considered “blue” for $B-V \leq 1$, and “red” for $B-V > 1$.

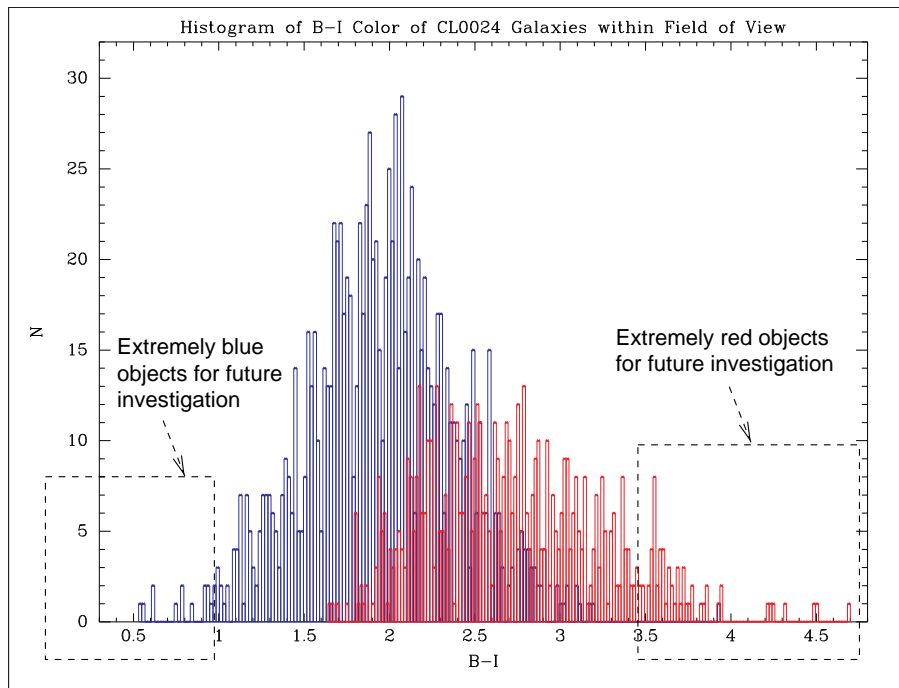


Figure 6: Histogram of the B-V color cut for galaxies in CL0024+1654. Since the color cut is made at $B-V=1$, the B-I color shows a different blue/red distribution. Objects with extreme colors are shown in dotted boxes.

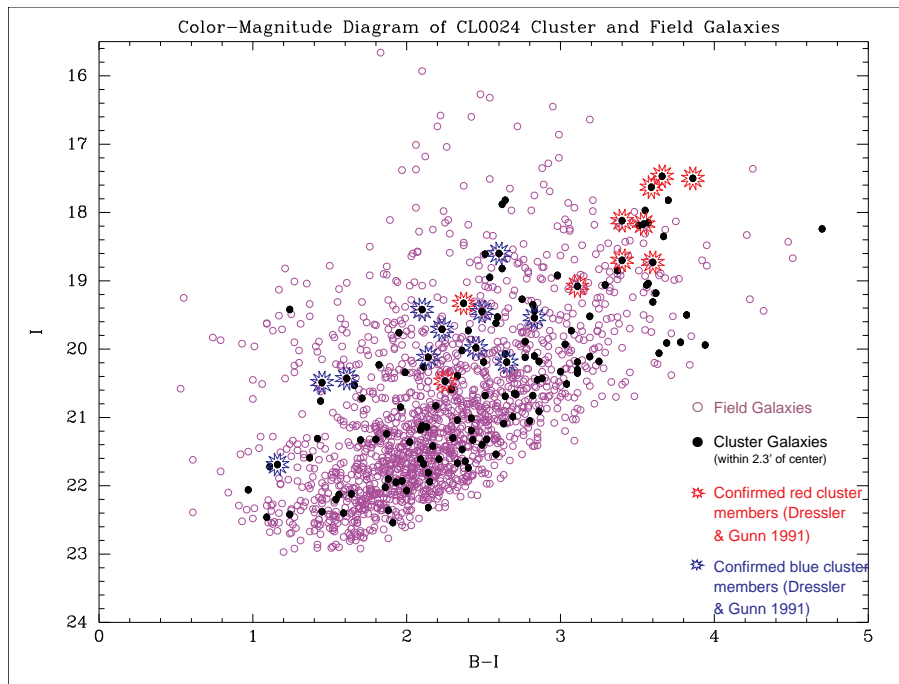


Figure 7: B-I vs I color magnitude diagram of the CL0024+1654 cluster and field galaxies. The field galaxies are plotted as open magenta circles; the cluster galaxies (within 2.3 arcmins of center) are plotted as closed black dots; confirmed cluster members are overlotted as red and blue open stars.

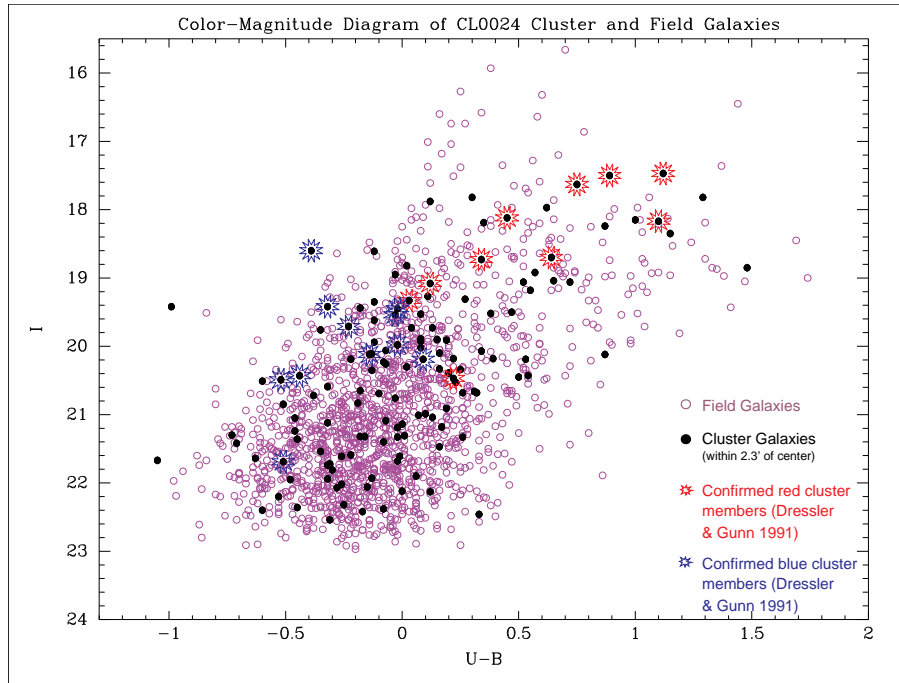


Figure 8: B-U vs U color magnitude diagram of the CL0024+1654 cluster and field galaxies. The field galaxies are plotted as open magenta circles; the cluster galaxies (within 2.3 arcmins of center) are plotted as closed black dots; confirmed cluster members are overplotted as red and blue open stars.

Table 3: Objects of Interest - “drop outs” for I band.

<i>Magnitude of I Band</i>	<i>Number of Objects</i>
≤ 20.0	9
≤ 21.0	36
≤ 22.0	106
≤ 23.0	234

to an old, quiescently evolving elliptical galaxy (e.g. NGC 3379).

The simulated $z = 0.4$ elliptical colors are well-matched to the bright, red galaxies seen in CL0024+1654. However, the bluest models at $z = 0.4$ do not appear to be good matches to the blue galaxies which are known to be cluster members. We can infer from this that these blue galaxies are photometrically unlike current-epoch galaxies at $z = 0$, most likely due to enhanced star formation rates. This effect has also been seen spectroscopically⁵. Turning to the galaxies within the “field” ($r > 2.3$ arcmins) with unknown redshifts, we can infer most are either foreground “field” galaxies or that there is a large galaxy population with unusual SEDs at the cluster redshift. The former conclusion seems more sound. Note that the “field” still contains a significant number of red objects which follow the $z = 0.4$ color track; this may indicate a supercluster in the CL0024+1654 field-of-view.

3.4 Optical band “drop-outs”: High-redshift candidates

A number of objects in the CL0024+1654 field-of-view had no flux in at least one filter bandpass while being detected in at least one other filter; these are commonly known as “drop-out” objects. Table 3 summarises the “drop-out” number as a function of I-band magnitude.

These objects are evenly distributed in the CL0024+1654 field of view. Most of these objects

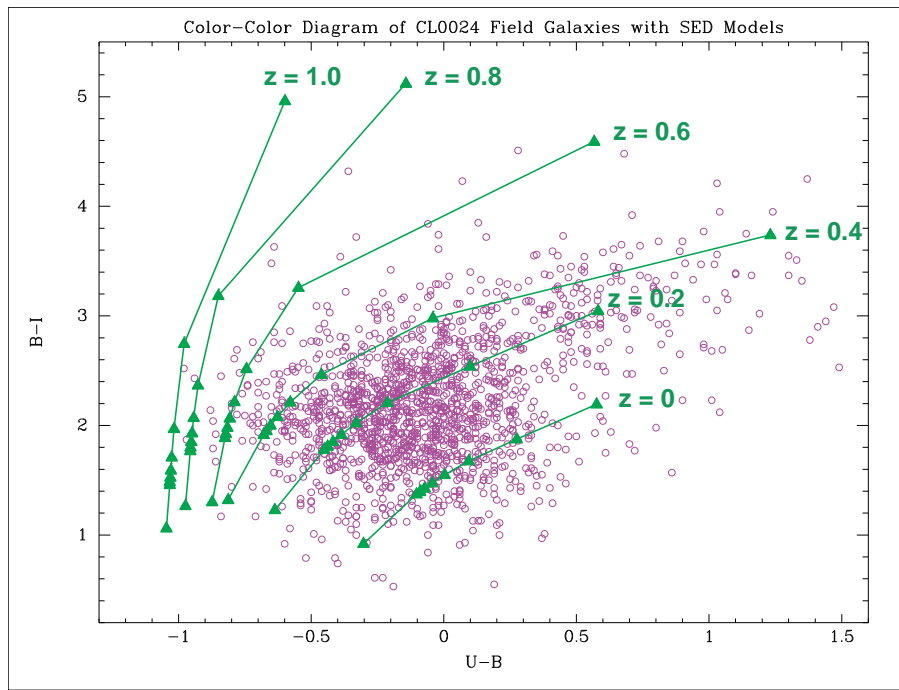


Figure 9: U-B vs B-I color-color diagram of CL0024+1654 field galaxies with SED Models overplotted for color redshift tracks $z=0.0, 0.2, 0.4, \dots, 1.0$.

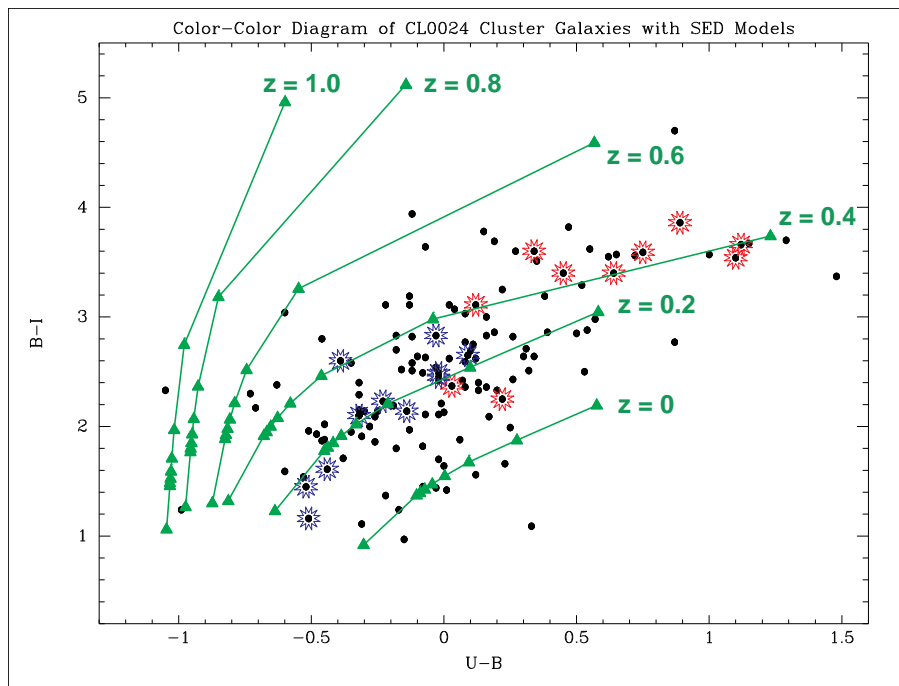


Figure 10: U-B vs B-I color-color diagram of CL0024+1654 center galaxies (within 2.3 arcmins of center) with SED Models overplotted for color redshift tracks $z=0.0, 0.2, 0.4, \dots, 1.0$. Confirmed cluster members are overplotted as red and blue open stars.

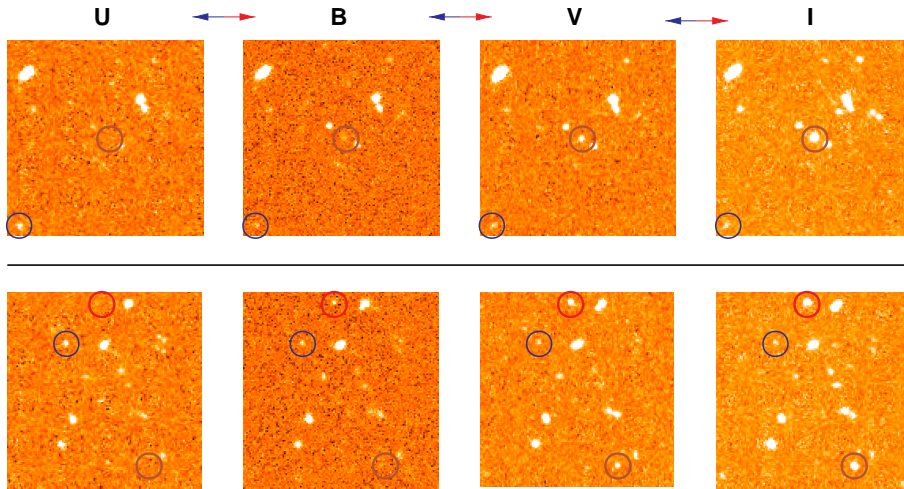


Figure 11: Two small sections of the CL0024+1654 are shown in U,B,V,I filters. The same set of objects are circled in all four frames; “red” circles indicate that the object gets redder, while “blue” circles indicate that the object gets bluer. Many such “drop out” objects were found throughout the CL0024+1654 field-of-view.

are “red”, i.e. they are brightest in the I-band. Example objects are shown in Figure 11, which presents two small sections of the CL0024+1654 field-of-view in 4 filters. The same object is circled in each filter. Sample “red” and “blue” objects are be traced in the four filters. The brightest 36 objects ($I \text{ mag} \leq 21.0$) were checked for M-star color characteristics⁷; only four likely M-stars were found. Given our one-sigma detection limits of $U \sim 27.0$ and $B \sim 27.5$, it seems certain that the rest of these objects are high-redshift galaxies candidates. A more detailed redshift estimate is pending.

4 Summary and a Look Ahead

In these proceedings, we have presented a preliminary analysis of a wide-field imaging survey of CL0024+1654. Based on this analysis, we have concluded that:

- CL0024+1654 appears to contain an intra-cluster faint blue galaxy population with photometric properties similar to the well-known field faint blue population;
- CL0024+1654 appears to be embedded in a larger super-cluster complex or filament;
- there are many high-redshift galaxy candidates in this field.

The next step is to more carefully define and study the galaxy sub-populations throughout this field. In particular, the bluest filters can be used to study UV-bright vs. UV-faint red galaxies. We also intend to do a more careful comparison of our photometric results with published spectroscopic results for the inner cluster galaxies to provide a more secure framework for interpreting the photometry of the field population.

5 Acknowledgments

This project was originally funded in 1993 by the REU summer student program at the National Optical Astronomy Observatories (NOAO), 950 North Cherry Avenue, P.O. Box 26732, Tucson, Arizona, USA. We thank the KPNO Director at that time for awarding us open-time for this project.

6 References

1. Bertin, E. *et al*, *A&A* **117**, 393 (1996).
2. Bruzual, A. *et al*, *ApJ* **405**, 538 (1993).
3. Czoske, O. *et al*, *CFHT Bulletin* **40**, 16 (1999).
4. Dressler, A. *et al*, *ApJS* **78**, 1 (1992).
5. Dressler, A. *et al*, *ApJS* **122**, 51 (1999).
6. Fort, B., Mellier, Y, Dantel-Fort, M., *A&A* **321**, 353 (1997)
7. Johnson, H.L. *et al*, *ARA&A* **4**, 193 (1966).